Gravitational-wave luminosity of binary neutron stars mergers

Francesco Zappa[1], Sebastiano Bernuzzi[1,2], David Radice[3,4], Albino Perego[2,1,5], and Tim Dietrich[6]
[1] *Dipartimento di Scienze Matematiche Fisiche ed Informatiche, Universitá di Parma, I-43124 Parma, Italia*
[2] *Istituto Nazionale di Fisica Nucleare, Sezione Milano Bicocca, gruppo collegato di Parma, I-43124 Parma, Italia*
[3] *Institute for Advanced Study, 1 Einstein Drive, Princeton, NJ 08540, USA*
[4] *Department of Astrophysical Sciences, Princeton University, 4 Ivy Lane, Princeton, NJ 08544, USA*
[5] *Dipartimento di Fisica, Università degli Studi di Milano Bicocca, Piazza della Scienza 3, 20126 Milano, Italia and*
[6] *Max Planck Institute for Gravitational Physics (Albert Einstein Institute), Am Mühlenberg 1, Potsdam-Golm, 14476, Germany*
(Dated: December 13, 2017)

We study the gravitational-wave peak luminosity and radiated energy of quasicircular neutron star mergers using a large sample of numerical relativity simulations with different binary parameters and input physics. The peak luminosity for all the binaries can be described in terms of the mass ratio and of the leading-order post-Newtonian tidal parameter solely. The mergers resulting in a prompt collapse to black hole have largest peak luminosities. However, the largest amount of energy per unit mass is radiated by mergers that produce a hypermassive neutron star or a massive neutron star remnant. We quantify the gravitational-wave luminosity of binary neutron star merger events, and set upper limits on the radiated energy and the remnant angular momentum from these events. We find that there is an empirical universal relation connecting the total gravitational radiation and the angular momentum of the remnant. Our results constrain the final spin of the remnant black-hole and also indicate that stable neutron star remnant forms with super-Keplerian angular momentum.

PACS numbers: 04.25.D-, 04.30.Db, 95.30.Sf, 95.30.Lz, 97.60.Jd

arXiv:1712.04267v1 [gr-qc] 12 Dec 2017

Gravitational waves (GWs) from a likely binary neutron star (BNS) inspiral have been observed for the first time on August 17th 2017 during the second observational run of Advanced LIGO and Virgo [1]. The observation sets a lower bound to the total radiated energy, $E_{\rm GW} > 0.025 {\rm M}_\odot {\rm c}^2$, by considering only a portion of the GW signal corresponding to the inspiral dynamics. The largest GW energy, however, is expected to be radiated during the merger and the subsequent postmerger phases [2, 3]. The only way to theoretically quantify the emitted GW energy is to perform numerical relativity (NR) simulations. NR-based models can be then evaluated on the intrinsic parameters of the binary esimated from the observations to obtain the emitted energy. In this work we study the GW peak luminosity and GW energy emitted by quasicircular binary neutron star mergers using one of the largest set of NR simulations currently available [2–13].

Compact binary mergers are the most powerful events in the Universe in terms of GW energy. The binary black hole (BBH) mergers observed so far emitted about $1{-}3\,{\rm M}_\odot\,{\rm c}^2$ with peak luminosities reaching $200\,{\rm M}_\odot {\rm c}^2\,{\rm s}^{-1}$ (about $\sim 3-4\times10^{56}\ {\rm erg\,s^{-1}}$) [14–16]. The largest luminosity is reached for an equal-masses and aligned spins configuration, with both holes spinning at maximum rate. Physically, spin-orbit interactions during the dynamics enhance the emission for the spin aligned configurations. Fits to the BBH luminosity and radiated energy as function of mass ratio and spins have been developed in a number of NR-based works, e.g. [17–20]. By constrast, the total radiated GW energy of BNS has been quantified only for particular cases, e.g. [3, 9, 10, 21], and quantitative models for predicting the properties of the merger remnant are missing.

We consider 100 different BNS simulations that include variation of the gravitational binary mass $M = M_A + M_B \in [2.4, 3.4]{\rm M}_\odot$, the mass ratio $q = M_A/M_B \in [1, 2.06]$, and a sample of 8 equations of state (EOSs) comprising 4 finite-temperature microphysical EOS models. Spin interactions in about 30 BNS are simulated consistently in general relativity following [22]. Spins are either aligned or antialigned to the orbital angular momentum, and of varying magnitude up to $|\mathbf{S}|/M^2 \approx 0.15$. A microphysical treatment of neutrino cooling is included in 37 simulations, following the method presented in [23]. Four simulations also included an effective treatment of turbulent angular momentum transport that may arise from small scale magnetohydrodynamical instabilities in the merger remnant [11]. Most of the BNSs are simulated at multiple grid resolutions for a total of more than 200 datasets, that guarantee control on numerical artifacts. Simulations are performed with the BAM [24] and THC codes [25]. Full details on the data are given elsewhere [26]. The GW energy $E_{\rm GW}$ and the binary's angular momentum J are calculated from our simulations from the GW multipolar waveform, as described in [2, 27]. We work with the mass and symmetric mass-ratio, $\nu = M_A M_B/M^2$, rescaled quantities, $e_{\rm GW} = E_{\rm GW}/(M\nu)$ and $j = J/(M^2\nu)$. The luminosity peak is computed as $L_{\rm peak} = \max_t \{dE_{\rm GW}(t)/dt\}$. Note

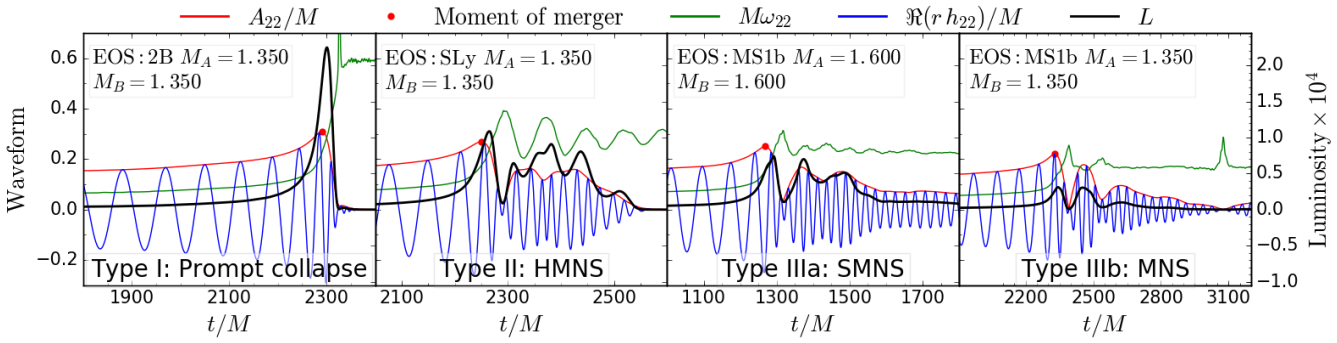

FIG. 1. Merger waveforms and GW luminosity for the three types of mergers. From left to right the GW correspond to a merger ending in: a prompt collapse to black hole (Type I), a hypermassive neutron star (Type II), a supramassive neutron star (Type IIIa) and a massive stable neutron star (Type IIIb). Note the double y-axis.

that, differently from BBH, the BNS luminosity does depend on the binary mass due to tidal interactions during the dynamics (see below). The conversion factor from geometric units $G = c = M_\odot = 1$ used here to CGS units is the Planck luminosity

$$L_P = \frac{c^5}{G} \approx 3.63 \times 10^{59}\ \mathrm{erg\,s^{-1}}\ ; \tag{1}$$

the typical order of magnitude of $L_{\rm peak}$ for compact binary mergers is $10^{-3} - 10^{-4} L_P$.

The BNS merger dynamics is crucially determined by tidal interactions [2, 3]. Ref. [2] has shown that $e_{\rm GW}$, j and many other key quantities at the moment of merger [1] can be fully characterized by the sum

$$\kappa_2^T = \kappa_2^{\rm A} + \kappa_2^{\rm B}\ , \tag{2}$$

of the gravitoelectric quadrupolar tidal polarizability coefficients [28]

$$\kappa_2^{\rm A} = 2\frac{X_B}{X_A}\left(\frac{X_A}{C_A}\right)^5 k_2^A\ . \tag{3}$$

Above, $k_2^{\rm A}$ is the quadrupolar Love number describing the static quadrupolar deformation of body A in the gravitoelectric field of the companion, C_A is the compactness, and $X_A = M_A/M$. The coefficient κ_2^T parametrizes at leading-order the tidal interactions in the general-relativistic 2-body Hamiltonian, waveform's phase and amplitude [29]. Larger energy emissions correspond to smaller values of κ_2^T, that, in turn, gets smaller values for larger masses, more compact NSs and softer EOS. In what follows we show that a similar characterization holds also for the peak luminosity.

The possible outcomes of a BNS merger are a prompt collapse to black hole (Type I), a hypermassive NS (HMNS, Type II), a supramassive NS (SMNS, Type IIIa), or a stable NS (MNS, Type IIIb) [30–32]. We find that the GW peak luminosity is reached during merger and the subsequent dynamical phase and it strongly depends on the merger type. For Type I mergers the luminosity peak just follows the moment of merger, similarly to the BBH case. Type II mergers have multiple peaks of comparable luminosity on a time scale of $\mathcal{O}(100M)$ (few ms). The peaks following the moment of merger are related to the HMNS emission and can be of comparable or stronger magnitude. Type III mergers are qualitatively similar to Type II, but the peak luminosities are lower. Four representative simulations are presented in Fig. 1.

The BNS peak luminosity can be characterized by a simple function of the tidal polarizability coefficients, Eq. (3). In the post-Newtonian (PN) description of the inspiral dynamics, tidal effects contribute to the luminosity with a leading order 5PN term $\delta L_{\rm Tidal} = \frac{32}{5}\nu^2 x^{10}\kappa_2^{\rm L}$ [33], where $x = (\pi M f_{\rm GW})^{2/3}$ is the PN expansion parameter, $f_{\rm GW}$ is the GW frequency and

$$\kappa_2^{\rm L} = 2\left[\frac{3 - 2X_A}{X_B}\kappa_2^A + (A \leftrightarrow B)\right]\ . \tag{4}$$

The perturbative parameter $\kappa_2^{\rm L}$ captures the strong-field dynamics behaviour for $L_{\rm peak}$ as shown in Fig. 2. Our irrotational BNS sample can be fit by [2]

$$L_{\rm peak}(\nu, \kappa_2^{\rm L}) \approx L_0 \frac{\nu^2}{q^2(\nu)} \frac{(1 + n_1\kappa_2^{\rm L} + n_2(\kappa_2^{\rm L})^2)}{(1 + d_1\kappa_2^{\rm L})}\ , \tag{5}$$

with $L_0 = 2.178 \times 10^{-2}$, $n_1 = 5.2(4) \times 10^{-4}$, $n_2 = -9.3(6) \times 10^{-8}$, $d_1 = 2.7(7) \times 10^{-2}$ and a coefficient of determination $R^2 = 0.943$. The maximal residuals are

[1] The moment of merger is formally defined as the time of the waveform amplitude's peak, that corresponds to the end of the chirp signal.

[2] Similar results are obtained also using κ_2^T since $X_A \sim X_B \sim 1/2$.

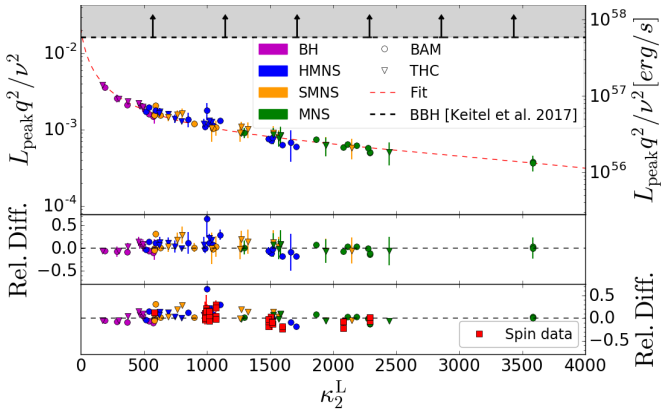

FIG. 2. GW luminosity peak as a function of the tidal parameter $\kappa_2^{\rm L}$. The errorbars are calculated from simulations performed at different resolutions. Second panel: fit's residuals with errors. Third panel: residuals of spin data compared to the fit.

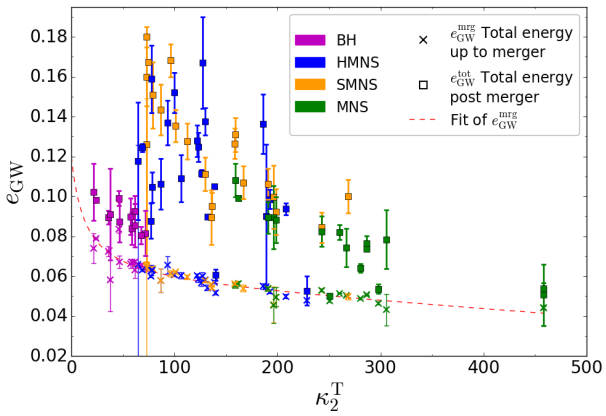

FIG. 3. Reduced GW energy at merger (×) and total (□) as a function of the tidal parameter $\kappa_2^{\rm T}$.

of the order of 30% (with one outlier at $\sim 60\%$). Note that the prediction using BBH fits would overestimate $L_{\rm peak}$ of, at least, a factor 4. Our fit also captures the spinning BNS data. For the spin magnitudes considered here, the spin-orbit contribution to $L_{\rm peak}$ is within the fit and numerical uncertainties. As an example of application, a fiducial equal-mass BNS with $M = 2.8{\rm M}_\odot$ and $\kappa_2^A = \kappa_2^B \sim 92$ ($\kappa_2^{\rm L} \sim 1472$) has $L_{\rm peak} \sim 8.168 \times 10^{-4}$ ($\sim 1.852 \times 10^{55}$ erg s^{-1}). The application of Eq. (5) to GW170817 is also straightforward and just requires to evaluate the posteriors for the likely distribution of the mass ratio the tidal parameters.

The $L_{\rm peak}$ analysis also highlights that the threshold between Type I and Type II mergers is approximately controlled by the value of $\kappa_2^{\rm L}$ (or $\kappa_2^{\rm T}$). Prompt collapse happens above a mass threshold $M > M_{\rm pc} = c_{\rm pc} M_{\rm max}^{\rm TOV}$, where $M_{\rm max}^{\rm TOV}$ is the maximum gravitational mass of a nonrotating NS and $1.3 \lesssim c_{\rm pc} \lesssim 1.6$ is a constant that depends only weakly on the binary's mass-ratio. Both $c_{\rm pc}$ and $M_{\rm max}^{\rm TOV}$ depend on the EOS [32, 34, 35]. For a given EOS, the prompt collapse threshold translates into limiting values of $\kappa_{2\ {\rm pc}}^{\rm T}$ (or $\kappa_{2\ {\rm pc}}^{\rm L}$), that can be computed by considering all the possible pairs of NS such that $M_A + M_B = M_{\rm pc}$ (with $1.1\ {\rm M}_\odot < M_{\rm A} < M_{\rm max}^{\rm TOV}$). For our set of 8 EOS we find that Type I mergers are characterized by $\kappa_{2\ {\rm pc}}^{\rm T} \sim 80$ ($\kappa_{2\ {\rm pc}}^{\rm L} \sim 600$) where the value can vary of about $\delta\kappa_{2\ {\rm pc}}^{\rm T} \lesssim 40$ ($\delta\kappa_{2\ {\rm pc}}^{\rm L} \lesssim 200$). Such predictions are verified by our NR sample, although no common threshold can be found for all the considered EOS.

The most luminous BNS do not correspond, in general, to the BNS that radiate the largest amount of energy. That is yet another difference with respect to BBH. The largest GW energies *per unit mass* are radiated by Type II mergers over typical timescales of few tens of milliseconds after the moment of merger [36]. The remnant HMNS undergoing gravitational collapse is a very efficient emitter of GWs; about two times the energy emitted during the inspiral and merger can be emitted during the postmerger phase. Figure 3 shows the total energy, $e_{\rm GW}^{\rm tot}$, and the energy irradiated up to the moment of merger, $e_{\rm GW}^{\rm mrg}$, as a function of $\kappa_2^{\rm T}$ for our irrotational BNS sample. While $e_{\rm GW}^{\rm mrg}$ tightly correlates with $\kappa_2^{\rm T}$, the total energy has a more complex behaviour. Our results set an upper bound of $e_{\rm GW}^{\rm tot} \lesssim 0.18$ obtained for $100 \lesssim \kappa_2^{\rm T} \lesssim 200$, e.g. for the fiducial $M = 2.8{\rm M}_\odot$ BNS discussed above. Hence, if two different BNSs with $M \sim 2.8{\rm M}_\odot$ and $\nu \sim 1/4$ are Type I and Type II respectively [3], then the former might be louder and the latter might emit more energy. Given similar total masses, Type II mergers can be louder of a factor $e_{\rm GW}^{\rm tot}({\rm Type\ II})/e_{\rm GW}^{\rm tot}({\rm Type\ I}) \sim 1.8$ with respect to Type I, and of a factor 3 with respect to Type III. However, not all Type II are louder then Type I. Sufficiently large individual NS masses in Type I mergers can rescale $e_{\rm GW}^{\rm tot}$ to larger absolute energies than those of Type II. The largest GW energy that a BNS can emit can be inferred from our dataset, we find

$$E_{\rm GW}^{\rm tot} \lesssim 0.126 \frac{M}{2.8}\ {\rm M}_\odot {\rm c}^2\ . \qquad (6)$$

Our results implies that current LIGO-Virgo GW searches at kiloHertz-frequencies are insensitive to the postmerger signal (Cf. Fig. 1 of [37]).

Finally, we show that the total radiated energy uniquely determines the angular momentum of the merger remnant, cf. Fig. 4. All the BNS remnants are characterized by values that lay on a given $e_{\rm GW}^{\rm tot}(j_{\rm rem})$ curve. That happens rather independendently from the binary's intrisinc parameters but also from the particular physics simulated in the postmerger. Notably, the simulations employing viscosity and neutrino cooling (marked

[3] For example if the NS matter is softer/stiffer in one case.

with stars in the plot) lay on the same curve of simulations employing a purely hydrodynamical prescription for the matter [11]. This fact suggests that the emission of gravitational radiation is the dominant mechanisms determining the dynamics on the dynamical timescales after merger, $T_{\rm dyn} \sim 20$ ms. The irrotational NR data are well described by the relation,

$$e^{\rm tot}_{\rm GW} \approx c_2 j^2_{\rm rem} - c_1 j_{\rm rem} + c_0 \ , \qquad (7)$$

where $c_0 = 0.9(4), c_1 = -0.4(3), c_2 = 0.05(3)$, with fit residuals below 20%. Spinning data increase fit residuals to 30%.

For Type I and II mergers, the final spin of the remnant black hole can be estimated from the angular momentum of the remnant system (BH or HMNS + disk) at the end of the initial, GW dominated phase. Thus, Eq. (7) could be used to estimate the final BH spin from the measurement of the energy radiated by the binary in GWs, which might be possible with third-generation GW observatories. The value of $J_{\rm rem}/M^2$ provides an upper limit for the remnant BH dimensionless spin, we predict $0.6 \lesssim J_{\rm rem}/M^2 \lesssim 0.9$ for moderatly spinning BNS. Type I mergers produce the smallest disks ($\sim 10^{-3}$M$_\odot$), carrying a negligible amount of angular momentum [12, 38–40]. Thus, the remnant and final BH angular momenta coincide and $0.75 \lesssim \left(J/M^2\right)_{\rm BH,Type\ I} \lesssim 0.8$, where the fastest spinning black holes are associated with larger values of $\kappa^{\rm L}_2$. For Type II mergers, we estimate that a disk of baryon mass $M_{b,\rm disk} \sim 0.1$ M$_\odot$ contains 10-15% of $J_{\rm rem}$. Viscosity-driven disk ejecta can carry away a large fraction of this momentum over the disk lifetime while we evaluate that $\Delta(J/M^2)_{\rm BH,Type\ II} \lesssim 0.03$ by accretion. For the final BH dimensionless spin we predict $0.6 \lesssim \left(J/M^2\right)_{\rm BH,Type\ II} \lesssim 0.85$, where the slowest spinning BHs are produced by light, symmetric BNSs.

The dimensionless angular momentum at the end of the initial, GW dominated, phase of the postmerger evolution for Type III binaries is in the range $0.62 \lesssim J_{\rm rem}/M^2 \lesssim 0.82$. We compare $J_{\rm rem}$ for each Type-III binary to that of sequences of uniformly rotating NSs having the same rest-mass. We find that $J_{\rm rem}$ exceeds, in most cases significantly, the Keplerian limit. Type III remnants are thus *super-Keplerian*. This suggests that the subsequent viscous evolution is likely to be accompanied by massive outflows [13, 41].

Acknowledgments We thank A. Nagar for comments. SB acknowledges support by the EU H2020 under ERC Starting Grant, no. BinGraSp-714626. DR acknowledges support from a Frank and Peggy Taplin Membership at the Institute for Advanced Study and the Max-Planck/Princeton Center (MPPC) for Plasma Physics (NSF PHY-1523261). Computations were performed on the supercomputer SuperMUC at the LRZ (Munich) under the project number pr48pu, on the supercomputers Bridges, Comet, and Stampede (NSF XSEDE allocation TG-PHY160025), on NSF/NCSA Blue Waters (NSF PRAC ACI-1440083), and on Marconi (PRACE proposal 2016153522 and ISCRA-B project number HP10B2PL6K).

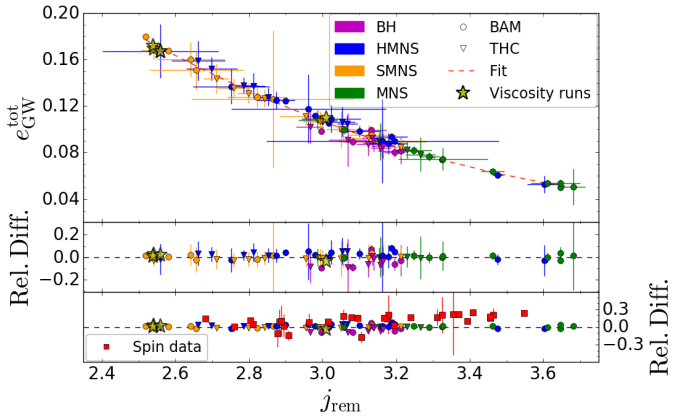

FIG. 4. Reduced total GW energy vs. final angular momentum of the remnant. Simulations including magnetically-driven viscosity effects [11] are marked with stars, the empty star refers to a control run with zero viscosity. Lower panels: residuals of the fit and the residuals of spin data, with errors.

[1] B. P. Abbott et al. (Virgo, LIGO Scientific), Phys. Rev. Lett. **119**, 161101 (2017), arXiv:1710.05832 [gr-qc].
[2] S. Bernuzzi, A. Nagar, S. Balmelli, T. Dietrich, and M. Ujevic, Phys.Rev.Lett. **112**, 201101 (2014), arXiv:1402.6244 [gr-qc].
[3] S. Bernuzzi, T. Dietrich, and A. Nagar, Phys. Rev. Lett. **115**, 091101 (2015), arXiv:1504.01764 [gr-qc].
[4] S. Bernuzzi, A. Nagar, T. Dietrich, and T. Damour, Phys.Rev.Lett. **114**, 161103 (2015), arXiv:1412.4553 [gr-qc].
[5] T. Dietrich, S. Bernuzzi, M. Ujevic, and B. Brügmann, Phys. Rev. **D91**, 124041 (2015), arXiv:1504.01266 [gr-qc].
[6] T. Dietrich and T. Hinderer, Phys. Rev. **D95**, 124006 (2017), arXiv:1702.02053 [gr-qc].
[7] T. Dietrich, S. Bernuzzi, and W. Tichy, (2017), arXiv:1706.02969 [gr-qc].
[8] D. Radice, S. Bernuzzi, W. Del Pozzo, L. F. Roberts, and C. D. Ott, Astrophys. J. **842**, L10 (2017), arXiv:1612.06429 [astro-ph.HE].
[9] T. Dietrich, M. Ujevic, W. Tichy, S. Bernuzzi, and B. Brügmann, Phys. Rev. **D95**, 024029 (2017), arXiv:1607.06636 [gr-qc].
[10] T. Dietrich, S. Bernuzzi, M. Ujevic, and W. Tichy, Phys. Rev. **D95**, 044045 (2017), arXiv:1611.07367 [gr-qc].
[11] D. Radice, Astrophys. J. **838**, L2 (2017), arXiv:1703.02046 [astro-ph.HE].
[12] D. Radice, A. Perego, and F. Zappa, (2017), arXiv:1711.03647 [astro-ph.HE].
[13] D. Radice, A. Perego, S. Bernuzzi, and L. F. Roberts, In Prep..
[14] B. P. Abbott et al. (Virgo, LIGO Scientific), Phys. Rev. Lett. **116**, 061102 (2016), arXiv:1602.03837 [gr-qc].

[15] B. P. Abbott et al. (Virgo, LIGO Scientific), Phys. Rev. Lett. **116**, 241103 (2016), arXiv:1606.04855 [gr-qc].

[16] B. P. Abbott et al. (VIRGO, LIGO Scientific), Phys. Rev. Lett. **118**, 221101 (2017), arXiv:1706.01812 [gr-qc].

[17] J. G. Baker et al., Phys. Rev. **D78**, 044046 (2008), arXiv:0805.1428 [gr-qc].

[18] D. Keitel et al., Phys. Rev. **D96**, 024006 (2017), arXiv:1612.09566 [gr-qc].

[19] X. Jimnez-Forteza, D. Keitel, S. Husa, M. Hannam, S. Khan, and M. Prrer, Phys. Rev. **D95**, 064024 (2017), arXiv:1611.00332 [gr-qc].

[20] J. Healy and C. O. Lousto, Phys. Rev. **D95**, 024037 (2017), arXiv:1610.09713 [gr-qc].

[21] L. Baiotti, B. Giacomazzo, and L. Rezzolla, Phys. Rev. **D78**, 084033 (2008), arXiv:0804.0594 [gr-qc].

[22] W. Tichy, Phys.Rev. **D84**, 024041 (2011), arXiv:1107.1440 [gr-qc].

[23] D. Radice, F. Galeazzi, J. Lippuner, L. F. Roberts, C. D. Ott, and L. Rezzolla, Mon. Not. Roy. Astron. Soc. **460**, 3255 (2016), arXiv:1601.02426 [astro-ph.HE].

[24] B. Brügmann, J. A. Gonzalez, M. Hannam, S. Husa, U. Sperhake, et al., Phys.Rev. **D77**, 024027 (2008), arXiv:gr-qc/0610128 [gr-qc]; M. Thierfelder, S. Bernuzzi, and B. Brügmann, Phys.Rev. **D84**, 044012 (2011), arXiv:1104.4751 [gr-qc].

[25] D. Radice, L. Rezzolla, and F. Galeazzi, Mon.Not.Roy.Astron.Soc. **437**, L46 (2014), arXiv:1306.6052 [gr-qc]; Class.Quant.Grav. **31**, 075012 (2014), arXiv:1312.5004 [gr-qc].

[26] T. Dietrich et al., In Prep..

[27] T. Damour, A. Nagar, D. Pollney, and C. Reisswig, Phys.Rev.Lett. **108**, 131101 (2012), arXiv:1110.2938 [gr-qc].

[28] T. Damour and A. Nagar, Phys. Rev. **D81**, 084016 (2010), arXiv:0911.5041 [gr-qc].

[29] T. Damour, A. Nagar, and L. Villain, Phys.Rev. **D85**, 123007 (2012), arXiv:1203.4352 [gr-qc].

[30] T. W. Baumgarte, S. L. Shapiro, and M. Shibata, Astrophys. J. **528**, L29 (2000), arXiv:astro-ph/9910565.

[31] K. Hotokezaka, K. Kyutoku, H. Okawa, M. Shibata, and K. Kiuchi, Phys.Rev. **D83**, 124008 (2011), arXiv:1105.4370 [astro-ph.HE].

[32] A. Bauswein, T. Baumgarte, and H. T. Janka, Phys.Rev.Lett. **111**, 131101 (2013), arXiv:1307.5191 [astro-ph.SR].

[33] T. Hinderer, B. D. Lackey, R. N. Lang, and J. S. Read, Phys. Rev. **D81**, 123016 (2010), arXiv:0911.3535 [astro-ph.HE].

[34] K. Hotokezaka, K. Kiuchi, K. Kyutoku, H. Okawa, Y.-i. Sekiguchi, et al., Phys.Rev. **D87**, 024001 (2013), arXiv:1212.0905 [astro-ph.HE].

[35] K. Hotokezaka, K. Kiuchi, K. Kyutoku, T. Muranushi, Y.-i. Sekiguchi, et al., Phys.Rev. **D88**, 044026 (2013), arXiv:1307.5888 [astro-ph.HE].

[36] S. Bernuzzi, D. Radice, C. D. Ott, L. F. Roberts, P. Moesta, and F. Galeazzi, Phys. Rev. **D94**, 024023 (2016), arXiv:1512.06397 [gr-qc].

[37] B. P. Abbott et al. (Virgo, LIGO Scientific), (2017), arXiv:1710.09320 [astro-ph.HE].

[38] M. Shibata and K. Taniguchi, Phys.Rev. **D73**, 064027 (2006), arXiv:astro-ph/0603145 [astro-ph].

[39] L. Rezzolla, L. Baiotti, B. Giacomazzo, D. Link, and J. A. Font, Class. Quant. Grav. **27**, 114105 (2010), arXiv:1001.3074 [gr-qc].

[40] M. Shibata, S. Fujibayashi, K. Hotokezaka, K. Kiuchi, K. Kyutoku, Y. Sekiguchi, and M. Tanaka, (2017), arXiv:1710.07579 [astro-ph.HE].

[41] S. Fujibayashi, K. Kiuchi, N. Nishimura, Y. Sekiguchi, and M. Shibata, (2017), arXiv:1711.02093 [astro-ph.HE].